AJNR

Language and Memory Network Alterations in Temporal Lobe Epilepsy: A Functional and Structural Connectivity Study

Alireza Fallahi, Mohammad-Reza Nazem-Zadeh, Narges Hosseini-Tabatabaei, Jafar Mehvari Habibabadi, Seyed-Sohrab Hashemi-Fesharaki and Hamid Soltanian-Zadeh

AJNR Am J Neuroradiol published online 12 March 2025
http://www.ajnr.org/content/early/2025/03/11/ajnr.A8737

ORIGINAL RESEARCH

Language and Memory Network Alterations in Temporal Lobe Epilepsy: A Functional and Structural Connectivity Study

Alireza Fallahi, Mohammad-Reza Nazem-Zadeh, Narges Hosseini-Tabatabaei, Jafar Mehvari Habibabadi, Seyed-Sohrab Hashemi-Fesharaki, and Hamid Soltanian-Zadeh

ABSTRACT

BACKGROUND AND PURPOSE: This study evaluated preoperative alterations and postoperative reorganization of the joint language-memory network (LMN) from the perspective of resting-state functional and structural connectivity in Temporal lobe epilepsy (TLE). Graph theory and machine learning approaches were employed to explore automatic lateralization.

MATERIALS AND METHODS: Resting-state fMRI and DTI data were obtained from 20 healthy subjects and 35 patients with TLE. Functional and structural connectivity were calculated within the LMN before and after temporal lobectomy. ANOVA was performed to identify significant connectivity differences between groups. Four local graph measures were extracted from functional and structural connectivity matrices. Standard feature selection techniques and genetic algorithm (GA) methods were applied to select the optimal features. Subsequently, the K-nearest neighbor, support vector machine (SVM), Naive Bayes, and logistic regression classification methods were used to classify healthy controls (HCs) and pre-surgical TLE groups, as well as pre-surgical left TLE (LTLE) and right TLE (RTLE) groups. Also, relationships between psychological scores and the selected features were evaluated using a linear regression method.

RESULTS: The results demonstrated increased functional and decreased structural connectivity in TLE patients before surgery. After surgery, significant connections revealed reduced functional connectivity and increased structural connectivity in TLE patients. Functional analysis identified the left parahippocampal region in LTLE and the right temporal regions in RTLE as key areas. Structural connectivity analysis showed that memory-related areas in the bilateral occipital region and the left language-related area were the origins of alterations. The GA method achieved the highest classification performance using SVM for fMRI and DTI graph measures, with accuracy rates of 97% and 88% for distinguishing LTLE from RTLE, and 93% and 87% for distinguishing TLE from HC, respectively. Moreover, a significant relationship was observed between the best-selected features and memory-assisted cognitive tests.

CONCLUSIONS: Pre-surgical functional hyperconnectivity and post-surgical hypoconnectivity and also newly observed bilateral post-surgical structural connectivity, highlighting functional and structural alterations in the LMN network. Additionally, the study underscores the potential of machine learning for TLE diagnosis and lateralization. A limited sample size, particularly in the post-surgical group was one of the constraints of this study.

ABBREVIATIONS: TLE=Temporal lobe epilepsy; LMN=Language-memory network; GA=Genetic algorithm; HC=Healthy controls; LTLE=Left TLE; RTLE=Right TLE; AUC=Area under the curve

Received month day, year; accepted after revision month day, year.

From the Department of Biomedical Engineering (Alireza.Fallahi.), Hamedan University of Technology, Hamedan, Iran; Department of Neurosciences, Addiction Studies & Neuroimaging (Mohammad-Reza Nazem-Zadeh), School of Advanced Technologies in Medicine, Medical School (Narges Hosseini-Tabatabaei), Tehran University of Medical Sciences, Tehran, Iran; Isfahan Neuroscience Research Center (Jafar Mehvari Habibabadi), Isfahan University of Medical Sciences, Isfahan, Iran; Pars Advanced Medical Research Center (Seyed-Sohrab Hashemi-Fesharaki), Pars Hospital, Tehran, Iran; CIPCE, School of Electrical and Computer Engineering (Hamid Soltanian-Zadeh), Faculty of Engineering, University of Tehran, Tehran, Iran; Department of Neurosciences (Mohammad-Reza Nazem-Zadeh), Monash University, Melbourne, VIC, Australia; Medical Image Analysis Lab., Departments of Radiology and Research Administration (Hamid Soltanian-Zadeh), Henry Ford Health System, Detroit, MI, USA.

The authors declare no conflicts of interest related to the content of this article.

Please address correspondence to Hamid Soltanian-Zadeh, PhD, School of Electrical and Computer Engineering, Faculty of Engineering, University of Tehran, North Kargar Ave, Tehran, 14399, Iran; e-mail: hszadeh@ut.ac.ir.

SUMMARY SECTION

PREVIOUS LITERATURE: Prior studies on TLE have shown varied results, with hypo and hyper-connectivity. The primarily affected regions in language-memory (LMN) related nodes include the hippocampus, parahippocampus, and posterior cingulum. This research suggests that alterations in LMN networks are more pronounced in left TLE (LTLE) patients compared to right TLE (RTLE) patients. Post-surgery, findings generally report a decrease in functional connectivity. Structural connectivity studies evidenced an improved LMN network in TLE patients after surgery. These studies provide foundational insights into the impact of TLE on brain networks. Machine learning approaches have been increasingly employed in TLE diagnosis and lateralization.

Copyright 2025 by American Society of Neuroradiology.

KEY FINDINGS: Functional hyper-connectivity in preoperative TLE and hypo-connectivity post-surgery are mostly related to the memory network, especially in the hippocampus and parahippocampus regions of both hemispheres. In terms of structural connections, there are bilateral memory node alterations before surgery, with new alterations emerging post-operatively, some involving the language-memory nodes.

KNOWLEDGE ADVANCEMENT: This study demonstrates a novel approach to understanding alterations in the memory-language networks of TLE patients and network reorganization post-surgery. It advances clinical lateralization, presurgical strategies, and rehabilitation planning. The application of machine learning has proven effective in diagnosing and classifying TLE, highlighting potential biomarkers.

INTRODUCTION

Temporal lobe epilepsy (TLE) is the most common type of symptomatic epilepsy. A primary cause of TLE is middle temporal lobe sclerosis, and treatment options include medications and surgery. Approximately 30% of TLE patients require surgery due to drug-resistant seizures [1]. Among the most prevalent cognitive deficits in TLE patients are episodic memory and verbal memory problems [2,3]. Although standard surgical procedures (such as anterior temporal lobectomy) are generally effective in eliminating seizures, TLE patients remain at risk for postoperative cognitive impairments that can impact their quality of life [4,5]. In addition to the clinical and psychological characteristics essential for preoperative evaluation, fMRI can predict postoperative cognitive function and decline [6]. Various fMRI brain mapping methods, including functional connectivity [7,8] and effective connectivity [9,10], have been employed for this purpose. Additionally, evidence suggests that DTI is reliable for detecting and assessing structural changes in temporal and frontal regions both preoperatively and intraoperatively [11]. By integrating resting state-fMRI and DTI, multimodal imaging offers a comprehensive perspective on functional and structural abnormalities in TLE, aiding in seizure localization[12], understanding disease mechanisms[13], and enhancing surgical planning[14].

Given the frequent episodic and verbal memory challenges faced by TLE patients, preoperative fMRI studies have largely concentrated on memory (episodic or verbal)[15] or language[16], often treating these domains independently. While such studies have shown promise in predicting surgical outcomes, they fall short of addressing the broader questions surrounding cognitive functionality[17]. Notably, the interaction between language and memory functions is pivotal in the lateralization of TLE. As a result, maintaining the functional integrity of both networks is essential for TLE patients. Moreover, TLE serves as a valuable model for studying the interplay between memory and language networks since the epileptogenic region is situated in the temporal lobe—a critical area for both functions[18]. Additionally, TLE is frequently associated with hippocampal atrophy[19]. The hippocampus, whose role in memory processes is well-documented[20,21], is increasingly recognized for its influence on language processing. This dual role underscores its significance in understanding the cognitive deficits observed in TLE patients[16,20,22,23]. Limited research has explored memory and language networks together [24,25]. However, these studies often rely on fMRI during specific tasks and focus solely on functional changes, overlooking structural alterations in these networks.

Conventional DTI and fMRI techniques often struggle to accurately identify epileptogenic regions, particularly in cases where structural abnormalities are absent. This highlights the growing necessity for advancements in machine-learning techniques[26,27]. These approaches are increasingly being utilized to analyze DTI/fMRI data for feature extraction, TLE diagnosis, and lateralization[28–30]. Among these, the graph-theoretical approach has emerged as a key tool for studying functional and structural connectivity in neuroscience [31,32]. This method excels at modeling and quantifying the brain as a complex network. Graph-theoretical metrics, which capture abnormalities in functional connectivity, have proven to be valuable markers for clinical diagnostics and for assessing disease progression. These approaches not only offer deeper insights into the neurobiological mechanisms of TLE but also show promise in improving diagnostic precision[33,34].

Here we hypothesized that TLE impacts distinct functional and structural alterations and that postoperative reorganization varies among TLE patients. Additionally, we hypothesized that graph measures construct a relevant feature space for a machine-learning approach to predict and lateralize TLE. To test these hypotheses, we investigated the joint language and memory networks. We leveraged resting-state fMRI data in conjunction with DTI to assess functional and structural alterations in these networks before and after surgery. Our approach involved graph theory for feature extraction, followed by genetic algorithm techniques for feature selection. We employed various classifiers to distinguish between healthy individuals and patients with TLE, encompassing both left and right TLE cases. We have also classified patients with left and right TLE.

MATERIALS AND METHODS

Study design

This study utilized a cross-sectional design to examine functional and structural connectivity in TLE patients compared to HCs using advanced imaging techniques.

Participants

In this study, resting-state fMRI and DTI images of 20 healthy control (HC) subjects and 35 patients with TLE (21 left TLE (LTLE) patients and 14 right TLE (RTLE) patients) of different ages were used. The data were acquired by a 3T Siemens scanner between 2019 and 2021. Ten patients underwent surgery and achieved an Engel class 1 outcome after 1 year, confirming the reliability of lateralization of TLE. Also, fMRI and DTI imaging with the same protocol were obtained from these patients after surgery. The demographic information of the studied subjects is given in Table 1. Also, the complete information on the patients studied in this research is given in Table S.1 of the Supplementary Materials. All subjects in the control group were medically healthy and had no neurological or psychiatric disorders at the time of the study. All subjects were asked to remain calm during the MRI scan, to close their eyes without falling asleep and not to

think about anything in particular. The Ethics Committee of Tehran University of Medical Sciences approved the study. The inclusion and exclusion criteria for patient selection, as well as the methods used for patient diagnosis, are detailed in the supplementary materials.

Table 1: Subjects characteristics

Characteristic	HC	LTLE	RTLE	P-Value
Sample size	20	21	14	-
Sex (M/F)	9/11	10/11	8/6	0.73‡
Age (yr), mean ± STD [range]	27.7± 4.2 [17-36]	31.9± 8.2 [17-54]	26.8± 6.2 [17-36]	0.059*
Onset Age (yr), mean ± STD [range]	-	10.8± 8.2 [0.5-29]	9.4± 9.4 [0.5-28]	0.6*

Note: (M/F): Male/Female- yr: Year- STD: Standard Deviation

‡ Fisher exact test

* Two-sample *t*-test

MRI Protocol and Preprocessing

The imaging data were acquired using a 3 Tesla Siemens (Magnetom Prisma) MRI scanner at the National Brain Mapping Lab. The fMRI data were captured using an EPI pulse sequence with a total duration of 990 seconds. The DTI data includes two series with b values of 1000 and 2000 s/mm2, respectively. The rs-fMRI data were preprocessed using the DPABI toolbox[35] (version 4.2, based on SPM12) and using standard procedure. The DTI data were initially preprocessed using FSL's EDDY[36] method (v3.19.0), and further analysis was performed using Explore-DTI[37] software (v4.6.8). More details of structural, functional, and DTI protocols and preprocessing stages were represented in supplementary materials.

Regions of Interest (ROIs) Definition

We used 74 symmetrical ROIs for the language-memory network (LMN) which were previously defined and validated [38] and extracted using the intrinsic connectivity atlas of homotopic regions[39]. These regions include 74 symmetrical regions in the left and right hemispheres (37 regions in each lobe). These regions were also classified based on their membership in a specific resting-state network. For this purpose, the 7 resting state network atlas defined by Yeo et al. [40] was used. Figure. 1 represents these ROIs. More details about the ROI definition are mentioned in the Supplementary Materials including Table S.2.

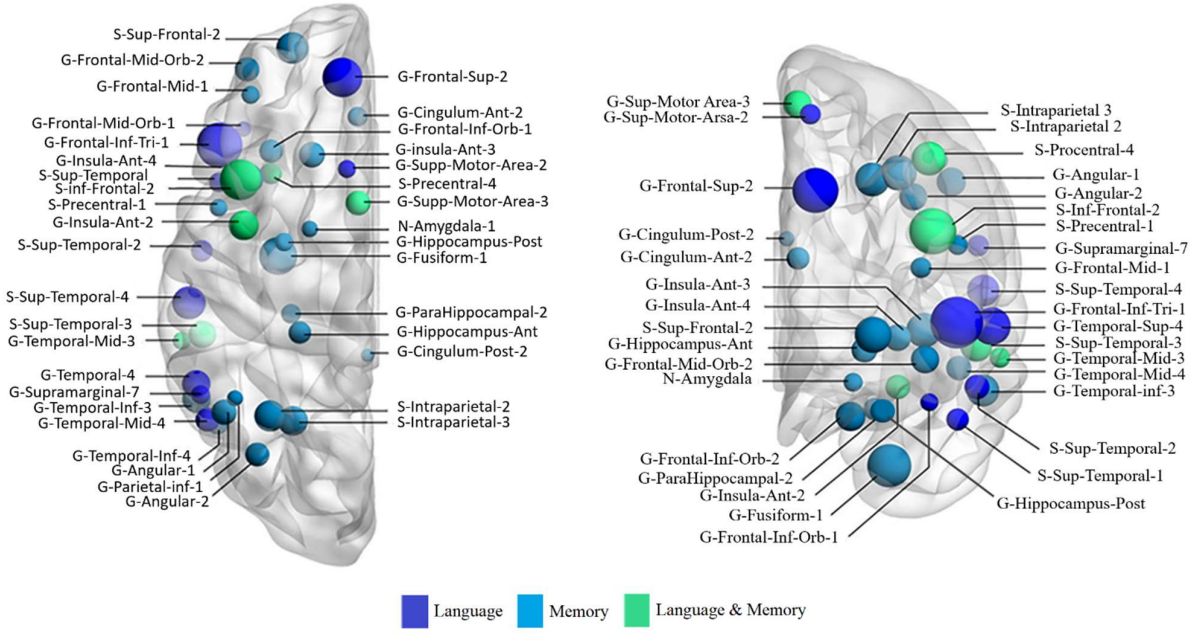

FIG 1: ROIs considered for the memory and language network along with the names of each area

Analysis of Graph Characteristics

To extract relevant features from connectivity matrixes with the classification purpose, we used the graph theoretical method. After preprocessing the fMRI and DTI data, blood oxygen level-dependent signals were extracted for the 74 regions. Functional connections were calculated using Pearson's correlation coefficient between the time series of each ROI pair. Structural connectivity was determined using the DTI images. Following the Fisher-Z transform, negative correlations in the connectivity matrices were set to zero for graph theory analysis. Additionally, spurious connections were removed using proportional thresholding on the connectivity matrices [41]. We chose a threshold of 0.2 as the proportional threshold to preserve the small-world property of real functional networks in the brain, based on previous studies [41]. Accordingly, we employed centrality measures to assess the complexity of functional connectivity. These measures included degree centrality, betweenness centrality, and closeness centrality, which have also been investigated in previous research [42]. Additionally, we utilized local efficiency to measure the local information processing capabilities within a larger network [43] as a fourth graph measure.

Feature Selection and Classification

To reduce the number of features we used two separate approaches for feature selection. The first was a standard feature selection process [44]. Firstly, we removed features with small standard deviations (below 0.01). Next, we excluded features whose correlation with the outcome was not significant (p-value < 0.05) using Pearson's correlation coefficient. Finally, To address multicollinearity, pairwise Pearson's correlation coefficients were used among the remaining features. For feature pairs with a correlation coefficient over 0.6, one feature was removed based on its relative strength of correlation with the outcome variable—specifically, we retained the feature that showed a higher correlation with the outcome.

The second approach involved using a genetic algorithm (GA) [45,46]. In this method, each graph feature is encoded as a genome, and a subset of selected features is considered a chromosome, represented by binary strings. Additional information about GA implementation was mentioned in supplementary materials.

We employed four classifiers, namely k-nearest neighbor, SVM, Naive Bayes, and logistic regression, to classify the HC and pre-operation TLE groups, as well as the pre-operation LTLE and RTLE groups. These classifiers were chosen based on their established effectiveness and complementary properties in analyzing medical data47,[48], particularly for small to medium-sized datasets with class imbalance, as is common in clinical studies and also epilepsy diagnosis[49],50.

Given the limited dataset size, we used the Leave-One-Out Cross-Validation method to ensure reliable results and mitigate issues such as overfitting. In this procedure, feature selection was performed independently within each fold to ensure the reliance of the process only on the training data. As a result, the selected feature set could vary between iterations depending on the data distribution in the training set. Following Leave-One-Out Cross-Validation, we determined the final set of features consistently selected across the majority of iterations, ensuring the robustness and interpretability of the final model.

The results were assessed using various classification evaluation metrics, including accuracy, sensitivity, F1-score, and area under the curve (AUC). Explanations of these metrics were provided in the supplementary material.

Psychological Tests

All participants completed an extensive set of cognitive assessments before surgery; 12 cognitive tests were used including; Logical Memory 1, Logical Memory 2, Verbal Paired Associate 1, Verbal Paired Associate 2, Auditory immediate memory, Visual immediate, Immediate memory, Auditory Delay, Visual delay, Auditory recognition, General Memory and Working memory [51,52]. We also applied regression analysis to evaluate the prediction of psychological scores with the selected graph measures. Support vector regression was applied to functional and structural selected graph measures to predict the psychological scores. Then, we calculated adjusted R^2, p-value, and mean squre error between the predicted and measured intelligence scores to identify the model performance. The full description of psychological tests was presented in the supplementary materials.

Statistical Analysis

For comparing the gender distribution (male/female) between LTLE, RTLE, and HC groups, we employed Fisher's exact test due to its suitability for categorical data and small sample sizes. For the mean age and age of onset, we used two-sample t-tests to evaluate differences in continuous variables across the two groups.

ANOVA test was used to compare the results between three HC, TLE before surgery, and TLE after surgery, as well as to compare the results between three HC, LTLE, and RTLE groups. Also, due to the multiple group comparisons and multiple regions, Bonferroni correction was applied to account for multiple comparisons, with adjusted p-values less than 0.05 considered statistically significant. This correction was specifically implemented for group comparisons, including preoperative LTLE, RTLE, and HC groups, postoperative LTLE, RTLE, and HC groups, as well as comparisons among preoperative TLE, postoperative TLE, and HC groups.

Reporting Guidelines

This study was conducted and reported following the STROBE (Strengthening the Reporting of Observational Studies) checklist to ensure comprehensive and transparent reporting of all observational study components.

RESULTS

Functional and Structural Connectivity Alterations in LMN

Our analysis revealed significant alterations in both functional and structural connectivity within LMN for preoperative and postoperative TLE patients. In preoperative TLE patients, functional connectivity was significantly increased across key nodes of the LMN, particularly in connections between the left and right posterior cingulum and the left and right intraparietal and precentral areas (Figure 2A; ANOVA, p-value<0.05, Bonferroni corrected). Specifically, RTLE patients exhibited increased intra-hemispheric connectivity within language-related regions, while LTLE patients demonstrated disrupted inter-hemispheric connectivity in memory-related networks (Figure 2B; ANOVA, p-value<0.05, Bonferroni corrected).

Post-surgically, a significant decrease in functional connectivity was observed in the hippocampal regions (Figure 2C; ANOVA, p-value<0.05, Bonferroni corrected). This reduction was more prominent in connections involving the left hippocampus of LTLE patients and bilateral memory regions in RTLE patients. Notably, this decline in connectivity was more pronounced in LTLE patients, reflecting substantial reorganization within memory networks.

Preoperatively, DTI metrics revealed significantly decreased mean FA in the TLE group compared to healthy controls, particularly in bilateral memory-related nodes within the parietal areas (Figure 3A; ANOVA, p-value<0.05, Bonferroni corrected). Specifically, connectivity reductions were more prominent in the left hemisphere of LTLE patients and bilateral in RTLE patients (Figure 3B).

Postoperatively, structural reorganization was evident for both LTLE and RTLE groups, with increased connectivity observed in memory-related tracts (Figures 3.C). These changes underscore adaptive structural adjustments in response to surgery.

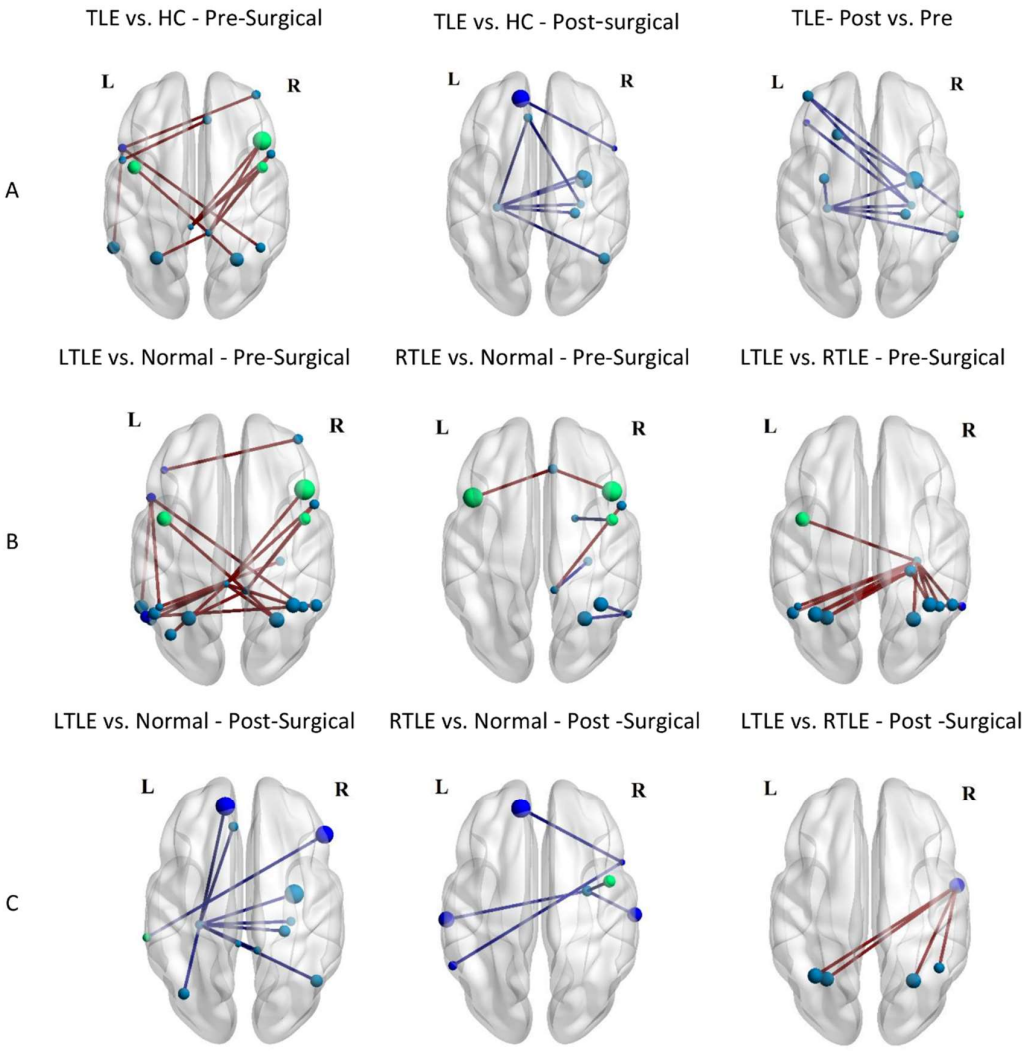

FIG 2: Significant functional connectivity differences (Bonferroni corrected p-value < 0.05) between HC and TLE groups before and after surgery: A) Between the HC and TLE groups before and after surgery; B) Between HC, LTLE, and RTLE groups before surgery. C) Between HC, LTLE, and RTLE groups after surgery. HC: Healthy control, TLE: Temporal lobe epilepsy, LTLE: Left temporal lobe epilepsy, RTLE: Right temporal lobe epilepsy.

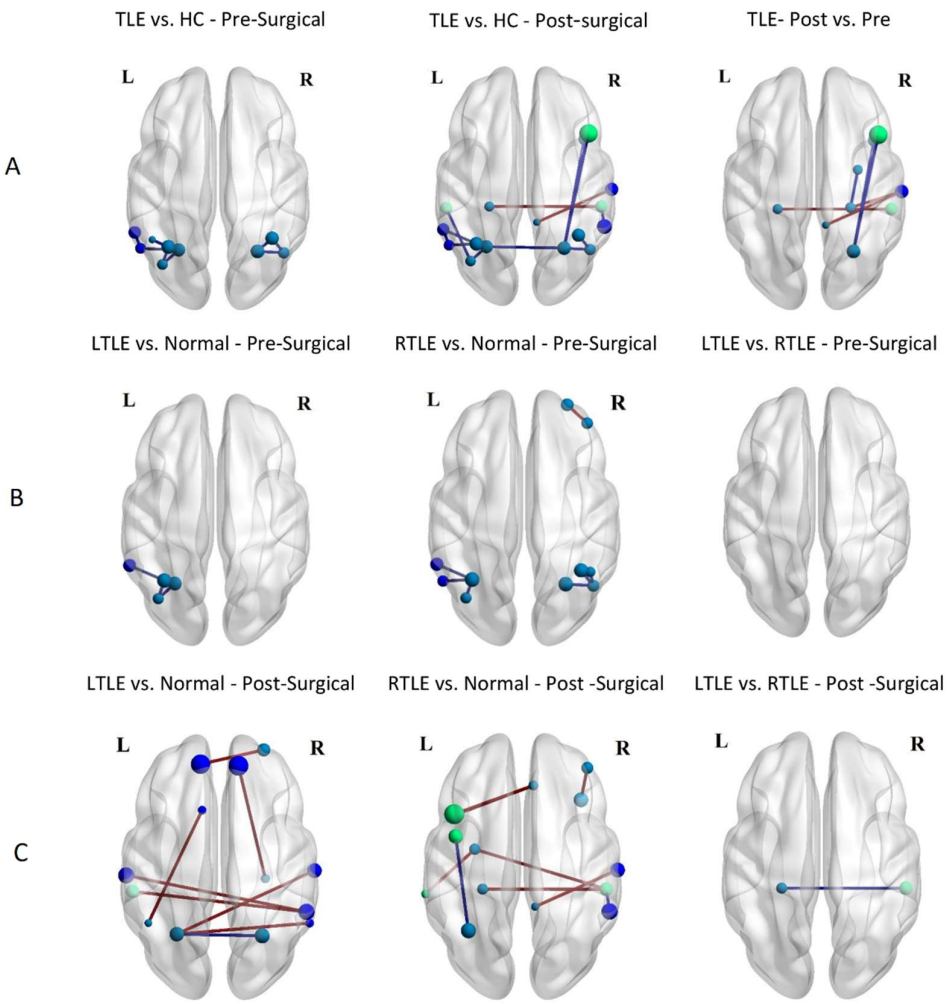

FIG 3: Significant structural connectivity differences (Bonferroni corrected p-value < 0.05) between HC and TLE groups before and after surgery: A) Between the HC and TLE groups before and after surgery; B) Between HC, LTLE, and RTLE groups before surgery. C) Between HC, LTLE, and RTLE groups after surgery. HC: Healthy control, TLE: Temporal lobe epilepsy, LTLE: Left temporal lobe epilepsy, RTLE: Right temporal lobe epilepsy.

TLE Graph Feature Selection and Classification

Using a standard feature selection method and pre-operative TLE group, we identified 7 and 8 selected features for fMRI and DTI graph measures, respectively, in the classification of LTLE and RTLE groups. Additionally, we found 10 and 15 selected features for the HC and TLE groups for fMRI and DTI graph measures, respectively. Figure 4 illustrates the fitness function value (SVM classification accuracy) for the GA method for different numbers of selected features in both fMRI and DTI graph measures. Notably, 10 features demonstrated the best performance in DTI graph measures, while 13 features exhibited optimal performance in fMRI graph measures. Based on these results, we selected 10 features for DTI graph measures and 13 features for fMRI graph measures using the GA method. (Table. S.3 and S.4 of supplementary material show the selection nodes.)

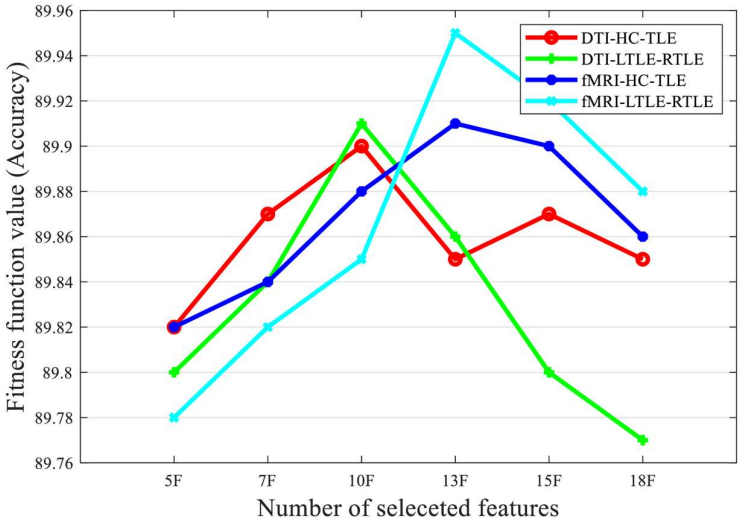

FIG 4: Fitness function value (SVM classification accuracy) for different numbers of selected features in the fMRI and DTI graph measures. SVM: Support vector machine.

Tables 2 and 3 present the classification results using selected graph measures based on standard feature selection and GA algorithms. Here, we compare the performance of HC vs. TLE groups and LTLE vs. RTLE groups. Using standard feature selection, the best accuracy achieved with fMRI and DTI graph measures for HC vs. TLE classification was 0.72 and 0.82, respectively. Similarly, for LTLE vs. RTLE classification, the best accuracy was 0.82 and 0.85 for fMRI and DTI graph measures, respectively.

The GA feature selection method yielded significantly higher accuracy compared to the standard method. For HC vs. TLE classification, the best accuracy achieved with fMRI and DTI graph measures was 0.93 and 0.87, respectively. Likewise, for LTLE vs. RTLE classification, the best accuracy was 0.97 and 0.87 for fMRI and DTI graph measures, respectively.

Table 2: Classification results using the graph measures selected by a standard feature selection algorithm.

		fMRI selected graph measures				DTI selected graph measures			
	Classifiers	**Bays**	**SVM**	**Logistic**	**K-nearest neighbor**	**Bays**	**SVM**	**Logistic**	**K-nearest neighbor**
HC vs. TLE	**Accuracy**	**0.72**	0.66	0.70	0.71	0.79	**0.82**	0.75	0.79
	sensitivity	0.82	0.88	0.76	0.70	0.79	0.91	0.79	0.81
	F1_score	0.79	0.77	0.76	0.72	0.75	0.86	0.81	0.75
	AUC	0.77	0.69	0.67	0.73	0.78	0.77	0.74	0.72
LTLE VS. RTLE	**Accuracy**	**0.82**	0.79	0.76	0.80	0.82	**0.85**	0.78	0.79
	sensitivity	0.85	0.75	0.78	0.79	0.90	1.00	0.75	0.78
	F1_score	0.85	0.81	0.79	0.81	0.84	0.87	0.79	0.76
	AUC	0.82	0.80	0.74	0.80	0.77	0.79	0.77	0.71

Note: AUC: Area under the curve

Table 3: Classification results using the graph measures selected by a GA feature selection algorithm.

		fMRI selected graph measures				DTI selected graph measures			
	Classifiers	**Bays**	**SVM**	**Logistic**	**K-nearest neighbor**	**Bays**	**SVM**	**Logistic**	**K-nearest neighbor**
HC vs. TLE	**Accuracy**	0.79	**0.93**	0.76	0.76	0.73	**0.87**	0.72	0.75
	sensitivity	0.74	0.97	0.80	0.76	0.79	1.00	0.76	0.79
	F1_score	0.75	0.94	0.81	0.76	0.73	0.91	0.78	0.74
	AUC	0.76	0.91	0.74	0.73	0.77	0.83	0.71	0.70
LTLE VS. RTLE	**Accuracy**	0.86	**0.97**	0.78	0.77	0.76	**0.88**	0.78	0.76
	sensitivity	0.86	0.95	0.81	0.76	0.75	1.00	0.70	0.75
	F1_score	0.88	0.98	0.83	0.76	0.73	0.91	0.79	0.73
	AUC	0.86	0.98	0.79	0.79	0.81	0.86	0.79	0.74

Note: AUC: Area under the curve

Relationship between Psychological Tests and Functional and Structural Connectivity

The results of the statistical comparison of the psychological test values between the LTLE and RTLE groups using the t-test method did not show any significant difference between the two groups with a significance level of 0.05 (p-value<0.05). As the best accuracy result related to GA-based selected features we only used these selected features for regression analysis.

These results show there is no significant relationship between the selected structural graph measures and these scores. Also, the results show the selected functional graph measures can predict verbal paired associates 2, immediate memory, and auditory delay ($r^2 = 0.53$, p-value = 0.01; $r^2 = 0.53$, p-value = 0.01; $r^2 = 0.47$, p-value = 0.02) (Figure 5).

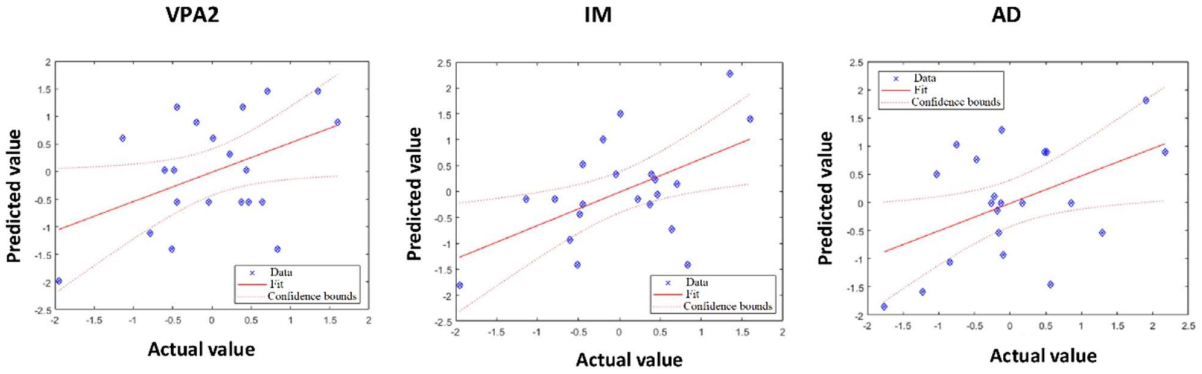

FIG 5: The regression lines with 95% confidence intervals for prediction of VPA2, IM, and AD (r2 = 0.53, p-value = 0.01- r2 = 0.53, p-value = 0.01- r2 = 0.47, p-value = 0.02). VPA2: Verbal Paired Associates, IM: Immediate Memory, and AD: Auditory Delay.

DISCUSSION

Functional connectivity evaluation

Comparing functional connectivity between the HC and TLE groups before surgery reveals significantly increased connectivity in the TLE group affecting memory and language-memory areas. While some prior studies have reported a decrease in functional connectivity among TLE patients, others have observed an increase in functional connections [25,53]. Our findings align with these studies, supporting the hypothesis that epileptic seizures are associated with heightened connectivity between neurons.

The left and right posterior cingulum are some main nodes that have significantly increased connections with the left and right intraparietal (memory network) and precentral area (language & memory). As the main role of the posterior cingulum in memory retrieval and consolidation these impairments show problems in spatial and episodic memory in TLE patients and also in joint language-memory abilities.

In post-surgery, the comparison of functional connectivity between the HC and TLE groups shows fewer significant changes in the functional connections. These connections have decreased in the TLE group and are mostly related to the memory network, particularly in the hippocampus and parahippocampus regions of both the left and right hemispheres. Given that the hippocampus and parahippocampus play crucial roles in language and memory networks, these results underscore the effect of surgery and highlight the potential side effects of temporal lobectomy on memory performance [6,25].

In a comparison of LTLE and RTLE functional connectivity groups with HC groups before surgery, our findings demonstrated more alterations in the LTLE vs. HC group compared with the RTLE vs. HC group. These alterations in the LTLE group showed hyperconnectivity compared with the HC group and related to bilateral parietal memory nodes and also bilateral frontal language & memory nodes. In the RTLE group, fewer significant connections were located in the right hemisphere. These connections show hypoconnectivity in memory nodes and hyperconnectivity in language & memory nodes. Our findings are consistent with previous research indicating that alterations in memory and language networks are more pronounced in LTLE patients compared to RTLE patients[25,29]. Also, the alteration of language & memory nodes in the precentral area both in LTLE and RTLE groups was interesting. After surgery, both LTLE and RTLE groups exhibited decreased functional connectivity compared to the HC group. In the LTLE group, significant connections related to memory nodes originate from the left parahippocampus, while in the RTLE group, significant connections related to language nods stem from bilateral temporal areas. These results highlight the impact of temporal lobectomy on brain function and emphasize the role of the hippocampus and parahippocampus in the memory network among TLE patients. The results also represent more post-surgical effects of memory function in LTLE and language function in RTLE groups.

Structural connectivity evaluation

The results of comparing structural connectivity between the TLE and HC groups before surgery reveal altered connections primarily associated with bilateral memory nodes in the parietal areas. Notably, the left hemisphere is more affected by these alterations. These changes are predominantly reduced in TLE patients compared to the Hc group, highlighting shifts in the structural connections of the memory network. In post-surgery, in addition to the pre-existing structural changes, new alterations emerge, some of which involve the language-memory nodes. Specifically, the increased structural connection between the left hippocampus and the right temporal lobe signifies the reorganization of the language and memory network after surgery. Comparing structural connectivity changes between the TLE patient group before and after surgery reveals an increase in structural connections between right language areas and left memory areas. Considering the right brain's impact on language function and the left brain's role in memory function, these changes suggest improved language and memory network function after surgery in TLE patients [11,54].

Comparing LTLE and RTLE groups before surgery, both exhibit structural changes related to the memory network region in the left parietal areas. Additionally, in the RTLE group, memory network regions in the right parietal areas undergo alterations. These findings indicate that RTLE patients are more affected by structural changes compared with LTLE patients before surgery. After surgery, more significant connections are observed in both LTLE and RTLE groups, with most connections showing an increase compared to the HC [8]. In the LTLE group, these connections are related to language and memory networks, while in the RTLE group, they are primarily associated with the memory network. These results underscore the more pronounced reorganization of the language network in left TLE patients after surgery. Another crucial point is that the increased connections occur bilaterally in both LTLE and RTLE groups.

Clinical significant

Our findings hold significant clinical implications for the management of TLE patients. The distinct functional and structural connectivity alterations observed in LTLE and RTLE groups provide valuable information for presurgical planning, helping to refine lateralization strategies and guide the selection of surgical approaches. Postoperatively, the observed changes in hippocampal and parahippocampal connectivity highlight the risk of memory and language impairments, suggesting a need for tailored neuropsychological assessments and rehabilitation protocols. Additionally, the increased structural connectivity between bilateral memory and language networks post-surgery reflects the brain's capacity for reorganization, opening avenues for targeted cognitive therapies to enhance these compensatory dynamics. Finally, the integration of graph-based classification models into clinical workflows offers a promising diagnostic tool to improve lateralization accuracy and inform individualized treatment strategies.

While the present study focuses on distant functional connectivity changes, findings from prior voxel-wise analyses in TLE provide complementary insights into local functional connectivity disruptions. Studies have shown localized alterations, particularly in the hippocampus, parahippocampus, and posterior cingulum—regions that play key roles in memory and language functions. Our results are consistent with the literature, as these regions are prominently implicated in the altered networks we observed. However, the distant connectivity approach employed in this work expands upon voxel-wise analyses by revealing network-wide changes in inter-regional communication, emphasizing the global reorganization of functional networks in TLE.

TLE Classification

The classification results for functional and structural graph features demonstrate acceptable accuracy in both LTLE and RTLE patients, as well as in the TLE and HC groups. Moreover, our results surpass those of previous studies [41,55] especially relied on graph features (undirected graphs). This advancement can significantly aid the surgeon in diagnosing the side of seizures in TLE patients. The selected features primarily relate to the Default Mode, Frontoparietal, and Dorsal Attention Networks. These networks play crucial roles in TLE patients [29].

Psychological Scores

Based on the results, there was no significant difference in psychological scores between LTLE and RTLE patients. Verbal Paired Associates, a parameter predicted using lateralized fMRI features as mentioned in previous studies, was affected in LTLE but not in RTLE patients [56]. Furthermore, our results demonstrate that certain psychological parameters can be predicted using the selected fMRI features. This suggests that fMRI features outperform DTI in estimating psychological parameters, which aligns with our classification findings.

Limitations

This study has some limitations. One of the main limitations is the relatively small sample size, especially in post-operative patients. From a statistical point of view, our analysis indicates sufficient statistical power to support the key findings and conclusions when comparing HCs with preoperative and postoperative TLE groups, as well as in comparisons between HCs, preoperative LTLE, and preoperative RTLE groups. However, we recognize that our analysis may have limited power for generalizability in comparisons involving HCs, postoperative LTLE, and postoperative RTLE groups.

While we acknowledge that increasing the sample size would improve the generalizability of our findings, we plan to address this limitation by prioritizing the expansion of the patient cohort, especially post-surgery patients, in future studies. This step will enable us to further validate and strengthen the implications of our research. Also, not all patients studied in this study underwent surgery, and therefore lateralization is not certain for some of them. In future studies, by increasing the number of post-operative patients this limitation may be overcome.

We followed a common practice of removing negative connections from the connectivity matrices according to previous studies[57,58]. Considering negative connections may provide relevant information about network organization but tends to decrease the reliability of global network properties and exclusion of negative correlations may simplify graph analysis offer clarity and stability in network properties and may overlook potentially meaningful interactions.

One of the key limitations of this study is the lack of validation using an independent or external dataset. While we employed leave-one-out cross-validation to train and evaluate our model, we acknowledge that training and testing on the same dataset — particularly with a sample size of 35 patients — may lead to overestimated predictive accuracy. This methodological choice was driven by logistical constraints, including differences in dataset compatibility and patient inclusion criteria. Future studies should aim to validate our findings using larger and more diverse datasets to confirm the generalizability of the proposed approach.

Besides reliable results of the GA algorithm in feature selection and classification accuracy examination of other feature selection methods may help to generalize this study which will be addressed in future studies.

CONCLUSIONS

This study highlights significant functional and structural connectivity alterations within the LMN of preoperative and postoperative TLE patients. Key findings revealed increased preoperative connectivity in regions such as the posterior cingulum and disrupted connections in memory and language networks, particularly between hemispheres. Post-surgical analyses demonstrated decreased hippocampal connectivity and structural reorganization, with distinct differences observed between LTLE and RTLE patients. These findings emphasize the critical role of network disruptions and reorganization in understanding TLE pathology. Specifically, our results highlight lateralized effects in memory and language regions, offering valuable insights into how surgical interventions impact these domains. Importantly, these findings have the potential to improve preoperative evaluation and postoperative outcomes in TLE patients by guiding personalized treatment strategies. Further, using machine learning-based analyses, this study recommends identifying potential biomarkers for TLE diagnosis and lateralization, which could enhance clinical decision-making.

ACKNOWLEDGMENTS

This work is based upon research funded by Iran National Science Foundation (INSF) under project No.4020796.

REFERENCES

1. Rubinger L, Chan C, D'Arco F, et al. Change in presurgical diagnostic imaging evaluation affects subsequent pediatric epilepsy surgery outcome. *Epilepsia*. 2016;57(1):32-40. doi:10.1111/epi.13229
2. Dutta M, Murray L, Miller W, Groves D. Effects of Epilepsy on Language Functions: Scoping Review and Data Mining Findings. *Am J Speech Lang Pathol*. 2018;27(1S):350-378. doi:10.1044/2017_AJSLP-16-0195
3. Fleury M, Buck S, Binding LP, et al. Episodic memory network connectivity in temporal lobe epilepsy. *Epilepsia*. Published online August 2022. doi:10.1111/epi.17370
4. Baxendale S, Thompson P. Red flags in epilepsy surgery: Identifying the patients who pay a high cognitive price for an unsuccessful surgical outcome. *Epilepsy & Behavior*. 2018;78:269-272. doi:10.1016/j.yebeh.2017.08.003
5. Audrain S, Barnett A, Mouseli P, McAndrews MP. Leveraging the resting brain to predict memory decline after temporal lobectomy. *Epilepsia*. 2023;64(11):3061-3072. doi:10.1111/epi.17767
6. Morgan VL, Rogers BP, González HFJ, Goodale SE, Englot DJ. Characterization of postsurgical functional connectivity changes in temporal lobe epilepsy. *J Neurosurg*. 2020;133(2):392-402. doi:10.3171/2019.3.JNS19350
7. Pravatà E, Sestieri C, Colicchio G, Colosimo C, Romani GL, Caulo M. Functional Connectivity MRI and Post-Operative Language

Performance in Temporal Lobe Epilepsy: Initial Experience. *Neuroradiol J*. 2014;27(2):158-162. doi:10.15274/NRJ-2014-10031
8. Foesleitner O, Sigl B, Schmidbauer V, et al. Language network reorganization before and after temporal lobe epilepsy surgery. *J Neurosurg*. 2021;134(6):1694-1702. doi:10.3171/2020.4.JNS193401
9. Vaudano AE, Mirandola L, Talami F, et al. fMRI-Based Effective Connectivity in Surgical Remediable Epilepsies: A Pilot Study. *Brain Topogr*. 2021;34(5):632-650. doi:10.1007/s10548-021-00857-x
10. Fallahi A, Hoseini-Tabatabaei N, Eivazi F, et al. Dynamic causal modeling of reorganization of memory and language networks in temporal lobe epilepsy. *Ann Clin Transl Neurol*. 2023;10(12):2238-2254. doi:10.1002/acn3.51908
11. Sainburg LE, Janson AP, Johnson GW, et al. Structural disconnection relates to functional changes after temporal lobe epilepsy surgery. *Brain*. 2023;146(9):3913-3922. doi:10.1093/brain/awad117
12. Fallahi A, Pooyan M, Habibabadi JM, Nazem-Zadeh MR. Comparison of multimodal findings on epileptogenic side in temporal lobe epilepsy using self-organizing maps. *Magnetic Resonance Materials in Physics, Biology and Medicine*. Published online 2021. doi:10.1007/s10334-021-00948-7
13. Chang YA, Marshall A, Bahrami N, et al. Differential sensitivity of structural, diffusion, and resting-state functional <scp>MRI</scp> for detecting brain alterations and verbal memory impairment in temporal lobe epilepsy. *Epilepsia*. 2019;60(5):935-947. doi:10.1111/epi.14736
14. Osipowicz K, Sperling MR, Sharan AD, Tracy JI. Functional MRI, resting state fMRI, and DTI for predicting verbal fluency outcome following resective surgery for temporal lobe epilepsy. *J Neurosurg*. 2016;124(4):929-937. doi:10.3171/2014.9.JNS131422
15. Limotai C, McLachlan RS, Hayman-Abello S, et al. Memory loss and memory reorganization patterns in temporal lobe epilepsy patients undergoing anterior temporal lobe resection, as demonstrated by pre-versus post-operative functional MRI. *Journal of Clinical Neuroscience*. 2018;55:38-44. doi:10.1016/j.jocn.2018.06.020
16. Whitten A, Jacobs ML, Englot DJ, et al. Resting-state hippocampal networks related to language processing reveal unique patterns in temporal lobe epilepsy. *Epilepsy & Behavior*. 2021;117:107834. doi:10.1016/j.yebeh.2021.107834
17. Roger E, Torlay L, Gardette J, et al. A machine learning approach to explore cognitive signatures in patients with temporo-mesial epilepsy. *Neuropsychologia*. 2020;142:107455. doi:10.1016/j.neuropsychologia.2020.107455
18. Drane DL, Pedersen NP. Knowledge of language function and underlying neural networks gained from focal seizures and epilepsy surgery. *Brain Lang*. 2019;189:20-33. doi:10.1016/j.bandl.2018.12.007
19. Thom M, Bertram EH. Temporal lobe epilepsy. In: ; 2012:225-240. doi:10.1016/B978-0-444-52898-8.00014-8
20. Moscovitch M, Cabeza R, Winocur G, Nadel L. Episodic Memory and Beyond: The Hippocampus and Neocortex in Transformation. *Annu Rev Psychol*. 2016;67(1):105-134. doi:10.1146/annurev-psych-113011-143733
21. Ranganath C, Ritchey M. Two cortical systems for memory-guided behaviour. *Nat Rev Neurosci*. 2012;13(10):713-726. doi:10.1038/nrn3338
22. Whitney C, Weis S, Krings T, Huber W, Grossman M, Kircher T. Task-dependent Modulations of Prefrontal and Hippocampal Activity during Intrinsic Word Production. *J Cogn Neurosci*. 2009;21(4):697-712. doi:10.1162/jocn.2009.21056
23. Piai V, Anderson KL, Lin JJ, et al. Direct brain recordings reveal hippocampal rhythm underpinnings of language processing. *Proceedings of the National Academy of Sciences*. 2016;113(40):11366-11371. doi:10.1073/pnas.1603312113
24. Banjac S, Roger E, Cousin E, et al. Mapping of Language-and-Memory Networks in Patients With Temporal Lobe Epilepsy by Using the GE2REC Protocol. *Front Hum Neurosci*. 2022;15. doi:10.3389/fnhum.2021.752138
25. Roger E, Pichat C, Torlay L, et al. Hubs disruption in mesial temporal lobe epilepsy. A resting-state fMRI study on a language-and-memory network. *Hum Brain Mapp*. 2020;41(3):779-796. doi:10.1002/hbm.24839
26. Sidhu MK, Duncan JS, Sander JW. Neuroimaging in epilepsy. *Curr Opin Neurol*. 2018;31(4):371-378. doi:10.1097/WCO.0000000000000568
27. Tsougos I, Kousi E, Georgoulias P, Kapsalaki E, Fountas KN. Neuroimaging methods in Epilepsy of Temporal Origin. *Current Medical Imaging Formerly Current Medical Imaging Reviews*. 2018;15(1):39-51. doi:10.2174/1573405613666170622114920
28. Yang Z, Choupan J, Reutens D, Hocking J. Lateralization of Temporal Lobe Epilepsy Based on Resting-State Functional Magnetic Resonance Imaging and Machine Learning. *Front Neurol*. 2015;6. doi:10.3389/fneur.2015.00184
29. Fallahi A, Pooyan M, Lotfi N, et al. Dynamic functional connectivity in temporal lobe epilepsy: a graph theoretical and machine learning approach. *Neurological Sciences*. Published online October 14, 2020. doi:10.1007/s10072-020-04759-x
30. Nazem-Zadeh MR, Elisevich K V., Schwalb JM, Bagher-Ebadian H, Mahmoudi F, Soltanian-Zadeh H. Lateralization of temporal lobe epilepsy by multimodal multinomial hippocampal response-driven models. *J Neurol Sci*. 2014;347(1-2):107-118. doi:10.1016/j.jns.2014.09.029
31. Vlooswijk MCG, Jansen JFA, Majoie HJM, et al. Functional connectivity and language impairment in cryptogenic localization-related epilepsy. *Neurology*. 2010;75(5):395-402. doi:10.1212/WNL.0b013e3181ebdd3e
32. Wilke C, Worrell G, He B. Graph analysis of epileptogenic networks in human partial epilepsy. *Epilepsia*. 2011;52(1):84-93. doi:10.1111/j.1528-1167.2010.02785.x
33. Carney PW. Lateralization of temporal lobe epilepsy based on resting-state functional magnetic resonance. 2015;6(August):1-9. doi:10.3389/fneur.2015.00184
34. Sone D, Beheshti I. Clinical Application of Machine Learning Models for Brain Imaging in Epilepsy: A Review. *Front Neurosci*. 2021;15. doi:10.3389/fnins.2021.684825
35. Yan CG, Wang XD, Zuo XN, Zang YF. DPABI: Data Processing & Analysis for (Resting-State) Brain Imaging. *Neuroinformatics*. 2016;14(3):339-351. doi:10.1007/s12021-016-9299-4
36. Andersson JLR, Sotiropoulos SN. An integrated approach to correction for off-resonance effects and subject movement in diffusion MR imaging. *Neuroimage*. 2016;125:1063-1078. doi:10.1016/j.neuroimage.2015.10.019
37. Leemans A, Jeurissen B, Sijbers J and JDK. ExploreDTI: a graphical toolbox for processing, analyzing, and visualizing diffusion MR data. In: *17th Annual Meeting of Intl Soc Mag Reson Med*. ; 2009.
38. Banjac S, Roger E, Pichat C, et al. Reconfiguration dynamics of a language-and-memory network in healthy participants and patients with temporal lobe epilepsy. *Neuroimage Clin*. 2021;31:102702. doi:10.1016/j.nicl.2021.102702
39. Joliot M, Jobard G, Naveau M, et al. AICHA: An atlas of intrinsic connectivity of homotopic areas. *J Neurosci Methods*. 2015;254:46-59. doi:10.1016/j.jneumeth.2015.07.013
40. Thomas Yeo BT, Krienen FM, Sepulcre J, et al. The organization of the human cerebral cortex estimated by intrinsic functional

connectivity. *J Neurophysiol*. 2011;106(3):1125-1165. doi:10.1152/jn.00338.2011
41. Gholipour T, You X, Stufflebeam SM, et al. Common functional connectivity alterations in focal epilepsies identified by machine learning. *Epilepsia*. 2022;63(3):629-640. doi:10.1111/epi.17160
42. Farahani F V., Karwowski W, Lighthall NR. Application of graph theory for identifying connectivity patterns in human brain networks: A systematic review. *Front Neurosci*. 2019;13(JUN):1-27. doi:10.3389/fnins.2019.00585
43. Zhou X, Zhang Z, Liu J, Qin L, Zheng J. Aberrant topological organization of the default mode network in temporal lobe epilepsy revealed by graph-theoretical analysis. *Neurosci Lett*. 2019;708(6). doi:10.1016/j.neulet.2019.134351
44. Devinsky O, Dilley C, Ozery-Flato M, et al. Changing the approach to treatment choice in epilepsy using big data. *Epilepsy & Behavior*. 2016;56:32-37. doi:10.1016/j.yebeh.2015.12.039
45. Maleki, Negar and Zeinali, Yasser and Niaki STA. A k-NN method for lung cancer prognosis with the use of a genetic algorithm for feature selection. *Expert Syst Appl*. 2021;164:113981.
46. Wutzl B, Leibnitz K, Rattay F, Kronbichler M, Murata M, Golaszewski SM. Genetic algorithms for feature selection when classifying severe chronic disorders of consciousness. Nakahara K, ed. *PLoS One*. 2019;14(7):e0219683. doi:10.1371/journal.pone.0219683
47. Almustafa KM. Classification of epileptic seizure dataset using different machine learning algorithms. *Inform Med Unlocked*. 2020;21:100444. doi:10.1016/j.imu.2020.100444
48. Abbasi B, Goldenholz DM. Machine learning applications in epilepsy. *Epilepsia*. 2019;60(10):2037-2047. doi:10.1111/epi.16333
49. Siddiqui MK, Morales-Menendez R, Huang X, Hussain N. A review of epileptic seizure detection using machine learning classifiers. *Brain Inform*. 2020;7(1):5. doi:10.1186/s40708-020-00105-1
50. Lima AA, Mridha MF, Das SC, Kabir MM, Islam MdR, Watanobe Y. A Comprehensive Survey on the Detection, Classification, and Challenges of Neurological Disorders. *Biology (Basel)*. 2022;11(3):469. doi:10.3390/biology11030469
51. Baxendale S, Wilson SJ, Baker GA, et al. Indications and expectations for neuropsychological assessment in epilepsy surgery in children and adults: Executive summary of the report of the <scp>ILAE</scp> Neuropsychology Task Force Diagnostic Methods Commission: 2017-2021. *Epilepsia*. 2019;60(9):1794-1796. doi:10.1111/epi.16309
52. Rodríguez-Cruces R, Bernhardt BC, Concha L. Multidimensional associations between cognition and connectome organization in temporal lobe epilepsy. *Neuroimage*. 2020;213:116706. doi:10.1016/j.neuroimage.2020.116706
53. Zhang Y, Zhang H, Chen X, et al. Strength and similarity guided group-level brain functional network construction for MCI diagnosis. *Pattern Recognit*. 2019;88:421-430. doi:10.1016/j.patcog.2018.12.001
54. Janson A, Sainburg L, Akbarian B, et al. Indirect structural changes and reduced controllability after temporal lobe epilepsy resection. *Epilepsia*. 2024;65(3):675-686. doi:10.1111/epi.17889
55. Hao S, Yang C, Li Z, Ren J. Distinguishing patients with temporal lobe epilepsy from normal controls with the directed graph measures of resting-state fMRI. *Seizure*. 2022;96:25-33. doi:10.1016/j.seizure.2022.01.007
56. Phuong TH, Houot M, Méré M, Denos M, Samson S, Dupont S. Cognitive impairment in temporal lobe epilepsy: contributions of lesion, localization and lateralization. *J Neurol*. 2021;268(4):1443-1452. doi:10.1007/s00415-020-10307-6
57. Wang JH, Zuo XN, Gohel S, Milham MP, Biswal BB, He Y. Graph Theoretical Analysis of Functional Brain Networks: Test-Retest Evaluation on Short- and Long-Term Resting-State Functional MRI Data. Kaiser M, ed. *PLoS One*. 2011;6(7):e21976. doi:10.1371/journal.pone.0021976
58. Karpychev V, Malyutina S, Zhuravleva A, et al. Disruptions in modular structure and network integration of language-related network predict language performance in temporal lobe epilepsy: Evidence from graph-based analysis. Epilepsy & Behavior. 2023;147:109407. doi:10.1016/j.yebeh.2023.109407

SUPPLEMENTAL FILES

Inclusion and exclusion criteria

The inclusion criteria for all TLE subjects will be: age 25 years to 45, diagnosis of localization-related epilepsy of mesial temporal lobe origin, epilepsy duration of at least 2 years, the onset of habitual seizures after the age of 2 years old, determined drug-resistant by the referring neurologist or epileptologist with failure of at least 2 antiepileptic drugs (AEDs) approved for monotherapy or adjunctive therapy for localization-related epilepsy, prolonged intracranial EEG studies completed in selected patients for lateralization of the epileptogenic focus, and candidate for surgical resection for the treatment of TLE.

People with TLE will be excluded if they are pregnant or lactating women, and/or have a history of serious cerebral insults after the age of 5 years, a progressive neurological disorder, mental retardation (I.Q. below 70), focal or lateralized neurological deficits other than memory disturbances or language dysfunction, habitual seizures that begin with auras which are not autonomic, psychic, olfactory, or gustatory, no postictal confusion following the complex partial seizure, previous EEG studies which showed generalized or extratemporal interictal epileptiform discharges, evidence of temporal neocortical or extratemporal lesions on neuroimaging, either CT or MRI, evidence of psychogenic non-epileptic seizures in addition to epileptic seizures, evidence of psychosis, and evidence of active substance or alcohol abuse or history of substance or alcohol abuse within two years of screening.

TLE diagnosis criteria

TLE was diagnosed based on the international league against epilepsy (ILAE) criteria and a comprehensive presurgical evaluation, including semiology, seizure history, neurologic examination, diagnostic magnetic resonance imaging (MRI), and electroencephalography (EEG). Standard diagnostic procedures were applied to diagnose left and RTLEs, including:

1. Seizure semiology was consistent with temporal lobe origin.
2. Temporal intermittent rhythmic delta and theta activity assessed by EEG and electrode localization of slow waves and spikes.
3. Evidence of mesial temporal sclerosis on MRI, such as altered hippocampal shape and volume on T1-weighted images, as well as changes in signal intensity on fluid-attenuated inversion recovery (FLAIR) imaging.

Each patient underwent a standard surgical resection. We categorized surgical outcomes for all patients based on the Engel classification one year after surgery. All patients in this study were seizure-free (Engel's I). Detailed information is summarized in Table 1. The Ethics Committee approved this project at the Tehran University of Medical Sciences, and all participants provided written informed consent to the Declaration of Helsinki.

Table S.1: Detail of TLE patients' demography

No	Frequency	Onset (years)	Handedness	Semiology (Salient Features)	Ictal EEG (LTM)	Epileptogenic Zone (LTM)	Irritative Zone (LTM)	MRI (MTS)	Laterality	Outcome
1	1-2/w	6	L	Behavioral arrest; right limb dystonia; right facial clonic activity (L)	Rhythmic theta activity L>R (T)	L (F<T)	L>R (F<T)	L	L	NA
2	3-4/m	8-9	R	Staring with oral automatisms; right limb dystonia (L)	Rhythmic theta activity L>R (F<T) Rhythmic delta activity L=R (T)	L (T)	R>L (F<T)	L	L	NA
3	2-3/m	10	R	Bilateral limb automatisms (T)	Rhythmic theta activity L>R (T)	L (T)	L=R	-	L	NA
4	1-4/m	8	R	Staring with oral automatisms (T)	Rhythmic theta activity L>R (T)	L (T)	L>R (F<T)	L	L	NA
5	-	16	R	Bilateral limb automatisms (T)	Rhythmic theta activity R (T)	R (T)	R (T)	R	R	NA
6	7-12/w	23	R	Staring with behavioral arrest; postictal aphasia (L)	Rhythmic theta activity L (T)	L (T)	L (T)	-	L	NA
7	-	13	R	Bilateral limb automatisms	Rhythmic theta activity L>R (T)	L=R (F<T)	(R>L) (T)	R	R	Engel I
8	1-4/m	0.5	R	Behavioral arrest with oral automatisms and blinking	Rhythmic theta activity L>R (F<T)	L (T)	R>L (F<T)	-	L	NA
9	1-4/m	0.3	R	Behavioral arrest with oral automatism	Rhythmic delta activity L>R (T)	L (T)	L	L	L	NA
10	7-12/w	13	R	Experiential aura; behavioral arrest; right limb dystonia (L)	Rhythmic theta activity L (T)	L (T)	R > L (T)	L	L	Engel I
11	0.3/m	2	L	Behavioral arrest with staring, oral automatisms, blinking	Rhythmic alpha & theta activity R>L (F<T) Rhythmic alpha activity R>L (T) with evolution to delta	R (T)	R=L (T>F)	R	R	NA
12	1/m	28	R	Behavioral arrest with oral automatisms; verbalization (R)	Rhythmic alpha & theta activity R (T>F)	R (T)	R>L (F<T)	R	R	NA
13	7-12/w	0.5	R	Behavioral arrest with staring, left limb automatisms; verbalization; ictal crying (R)	Rhythmic theta activity L>R (T>P)	L (T)	R=L (T)	R	R	NA

14	4-7/m	3	R	Left versive motion with left facial and limb clonic activity; vocalization (R)	Rhythmic theta activity R>L (T)	R (T)	R (T>F)	R	R	Engel I
15	4/m	0.6	R	Behavioral arrest with staring; right limb dystonia; verbalization	Rhythmic delta activity R (T>F), L (T) Rhythmic theta activity R (T) Rhythmic delta activity L>R (T)	R (T)	R (T)	R	R	Engel I
16	0.3-1/m	22	R	Left versive motion; left limb dystonia (R)	Rhythmic alpha activity R>L (T)	R (T)	R (T)	R	R	Engel I
17	2-3/m	14	R	Behavioral arrest with staring	-	L (T)	-	L	L	NA
18	4/w	3	R	Staring with oral automatisms; right versive motion, right facial clonic activity (L)	Rhythmic theta activity L>R (T)	L (T)	-	L	L	Engel I
19	7-12/w	15	R	Staring with blinking; left versive motion; left limb clonic activity; right facial; right limb clonic, right versive motion	Rhythmic delta activity R>L (T>P), L>R (T)	R>L (T>F)	L=R (T)	-	R	NA
20	0.25/m	13	Both	Behavioral arrest with staring	-	-	R=L (T)	L	L	NA
21	-	-	R	Behavioral arrest with staring	-	L>R (T>F)	-	-	L	NA
22	-	-	-	Bilateral limb automatisms (T)	-	R (T)	-	R	R	NA
23	1-4/m	11	R	Behavioral arrest with blinking and oral automatisms	Rhythmic theta activities L >R (T)	-	L	L	L	Engel I
24	1-4/w	19	R	Behavioral arrest; left limb automatism, right versive motion (L)	Rhythmic theta activity L>R (T)	L (T)	L (T)	L	L	NA
25	-	-	-	Behavioral arrest with staring	-	L (T)	-	-	L	NA
26	-	-	-	Behavioral arrest with staring	-	L (T)	-	-	L	Engel I
27	1-12/m	1	R	Behavioral arrest with oral automatisms; left limb automatisms; right limb automatisms	Rhythmic delta activity R>L (T>F) Rhythmic theta activity R (T)	R (T)	R > L (T)	R	R	NA
28	7-12/m	4	L	Experiential aura; behavioral arrest; Right Arm Dystonia	Rhythmic theta activities L>R (T)	L (T)	L (T)	L	L	NA
29	1-15/m	2-3	R	Behavioral arrest with blinking; left limb dystonia; ictal laughter (R)	Rhythmic alpha activity R>L (T)	R (T)	R (T)	R	R	Engel I
30	1-4/w	17	R	Behavioral arrest; left versive motion; oral automatisms (R)	Rhythmic theta activity R (T)	R (T)	(R > L) (T)	R	R	NA
31	3-12/m	7	R	Staring with oral automatisms; right limb dystonia	Rhythmic theta activity L>R (T). Bilateral rhythmic delta activity L=R (T)	(L>R) (T)	(L>R) (T>F)	-	L	NA

32	2-3/w	2	R	Behavioral arrest with staring and oral automatism, spitting; left limb dystonia	Rhythmic theta R>L (T) Rhythmic delta R>L (T>F)	R (T)	(R>L) (T)	R>L	R	Engel I
33	1-4/m	29	R	Behavioral arrest with oral automatisms; left limb automatisms	Rhythmic alpha L>R (T>F) Rhythmic theta activity L>R (T)	L (T)	L (T)	L	L	NA
34	0.3/m	14	R	Behavioral arrest with staring (T)	Rhythmic theta activity L>R (T)	L (T)	-	L	L	NA
35	0.3/m	18	R	Experiential aura	-	L (T)	L (T)	-	L	NA

MTS: Mesial Temporal Sclerosis.

MRI Protocol

The imaging data were acquired using a 3 Tesla Siemens (Magnetom Prisma) MRI scanner at the National Brain Mapping Lab. The fMRI data were captured using an EPI pulse sequence with TR = 3000ms, TE = 30s, flip angle = 90°, matrix size = 640 × 640, slice thickness = 2.4 mm, number of slices = 53, and a whole duration of 990 s (330 volume). Each head volume included 34 slices with a 64x64 matrix.

The DTI data includes two series with b values of 1000 and 2000 s/mm2, respectively. Each series consisted of 64 diffusion-weighted volumetric images and 5 reference volumes obtained with b0 s/mm2 for distortion correction. Other DWI parameters were as follows: TR = 9600 ms, TE = 92 ms, flip angle = 90°, matrix size = 880 × 880, slice thickness = 2.4 mm, and a total of 64 slices. Also, the structural data was collected using an MPRAGE pulse sequence with TR = 1840 ms, TE = 2.43 ms, acquisition matrix = 224x224, and an isotropic resolution of 1 mm.

Preprocessing of Imaging Data

The rs-fMRI data were preprocessed using the DPABI toolbox (version 4.2, based on SPM12). Standard steps, including removing the first ten samples, correcting the slice time, and realigning using a six-parameter (rigid-body) spatial transformation, were performed. Additional preprocessing steps include skull removal, head motion correction, image segmentation into white matter, gray matter, and cerebrospinal fluid (CSF), spatial normalization to standard space (MNI), and filtering using a Gaussian filter with a width of 4 mm (FWHM). Band-pass filtering (0.1 Hz < f < 0.01 Hz) was performed to reduce the influence of low-frequency drift and physiological signals related to breathing and cardiac activity.

The diffusion tensor data were initially preprocessed using FSL's EDDY method (v3.19.0), which improves the detection of outliers and removes noise caused by subject motion using Explore-DTI software (v4.6.8), we performed DTI-based tractography for the whole brain using a deterministic approach. The direction of the local device was determined by the principal eigenvector of the diffusion tensor, leveraging efficient algorithms. The processing was performed for a fiber length range of 10-500 mm, an angle threshold of 30 degrees, and a fractional anisotropy (FA) range of [0.2-1]. Next, the connection matrix (74x74) between the nodes was obtained using Explore-DTI software (v4.6.8). The FA value of each fiber was determined by considering the average FA values of all voxels in the fiber path. We performed 1,000,000 simple initial tracking points, each iteration having a unique instance of the parameter combination.

For post-operative patients, considering the structural changes resulting from surgery, we applied registration and normalization to a standard brain template during the preprocessing stage. This process was conducted prior to defining ROIs in both structural and functional images, ensuring proper alignment across patients and minimizing discrepancies caused by postoperative alterations. By implementing this approach, we were able to address these challenges effectively while maintaining the integrity of our analysis.

.

Definition of Regions of Interest (ROIs)

We used 74 symmetrical ROIs for the language-memory network (LMN) which were previously defined and validated (Banjac et al., 2021). In (Roger et al., 2020), the LMN regions were extracted using the intrinsic connectivity atlas of homotopic regions (AICHA) (Joliot et al., 2015). These regions include 72 symmetrical regions in the left and right hemispheres (36 regions in each lobe). Despite the standard lateralization of the language network, in this network, the nodes are considered in both hemispheres because language reorganization in TLE patients can be interhemispheric (Baciu & Perrone-Bertolotti, 2015) and also involves the non-dominant hemisphere in healthy subjects. Furthermore, since different reorganization patterns for anterior and posterior hippocampal networks have been reported, in addition to the areas considered in (Roger et al., 2020), Banjac et al (Banjac et al., 2021) separated the hippocampus into anterior and

posterior parts, obtaining 74 symmetrical areas in the left and right hemispheres (37 areas in each lobe). We used these 74 symmetrical ROIs to investigate the combined memory and language network. These regions were also classified based on their membership in a specific resting-state network. For this purpose, the 7 resting state network atlas defined by Yeo et al. (Thomas Yeo et al., 2011) was used. Table S.2 of the Supplementary Materials shows the details of the ROIs, including their names, coordinates, networks, and the MNI locations. Fig. 1 shows the ROIs we used for our LMN network analysis.

Table S.2: **74 LMN ROIs details**

Num	Region Name		LMN	NTW	MNI Coordinate			Hem	Lobe
					x	y	z		
1	G_Frontal_Sup-2-L	FS2L	L	DMN	-12	47	40	Left	Front
2	G_Frontal_Sup-2-R	FS2R	L	DMN	12	46	41	Right	Front
3	S_Sup_Frontal-2-L	SF2L	M	FPN	-27	56	1	Left	Front
4	S_Sup_Frontal-2-R	SF2R	M	FPN	28	56	7	Right	Front
5	G_Frontal_Mid-1-L	FM1L	M	FPN	-40	41	20	Left	Front
6	G_Frontal_Mid-1-R	FM1R	M	FPN	41	44	13	Right	Front
7	S_Inf_Frontal-2-L	IF2L	LM	FPN	-43	15	29	Left	Front
8	S_Inf_Frontal-2-R	IF2R	LM	FPN	44	19	28	Right	Front
9	G_Frontal_Inf_Tri-1-L	FIT1L	L	DMN	-49	26	5	Left	Front
10	G_Frontal_Inf_Tri-1-R	FIT1R	L	DMN	50	29	5	Right	Front
11	G_Frontal_Mid_Orb-2-L	FMO2L	M	FPN	-41	49	-5	Left	Front
12	G_Frontal_Mid_Orb-2-R	FMO2R	M	FPN	40	50	-4	Right	Front
13	G_Frontal_Inf_Orb-1-L	FIO1L	L	DMN	-42	31	-17	Left	Front
14	G_Frontal_Inf_Orb-1-R	FIO1R	L	DMN	44	33	-14	Right	Front
15	G_Frontal_Inf_Orb-2-L	FIO2L	M	LIMB	-21	23	-21	Left	Front
16	G_Frontal_Inf_Orb-2-R	FIO2R	M	LIMB	21	22	-20	Right	Front
17	S_Precentral-1-L	P1L	M	DAN	-50	6	26	Left	Front
18	S_Precentral-1-R	P1R	M	DAN	50	10	24	Right	Front
19	S_Precentral-4-L	P4L	LM	DAN	-42	1	49	Left	Front
20	S_Precentral-4-R	P4R	LM	FPN	44	1	48	Right	Front
21	G_SupraMarginal-7-L	SM7L	L	DMN	-55	-52	26	Left	Prtl
22	G_SupraMarginal-7-R	SM7R	L	DMN	55	-46	33	Right	Prtl
23	G_Angular-1-L	A1L	M	DMN	-48	-57	43	Left	Prtl
24	G_Angular-1-R	A1R	M	DMN	51	-52	43	Right	Prtl
25	G_Angular-2-L	A2L	M	DMN	-38	-70	39	Left	Prtl
26	G_Angular-2-R	A2R	M	DMN	45	-62	36	Right	Prtl
27	G_Parietal_Inf-1-L	PI1L	M	FPN	-45	-53	49	Left	Prtl
28	G_Parietal_Inf-1-R	PI1R	M	FPN	43	-53	48	Right	Prtl
29	S_Intraparietal-2-L	I2L	M	FPN	-34	-58	45	Left	Prtl
30	S_Intraparietal-2-R	I2R	M	DAN	37	-52	48	Right	Prtl
31	S_Intraparietal-3-L	I3L	M	DAN	-27	-60	43	Left	Prtl
32	S_Intraparietal-3-R	I3R	M	DAN	27	-61	46	Right	Prtl
33	G_Insula-anterior-2-L	IA2L	LM	DMN	-34	17	-13	Left	Insl
34	G_Insula-anterior-2-R	IA2R	LM	DMN	35	18	-13	Right	Insl
35	G_Insula-anterior-3-L	IA3L	M	SAL	-34	24	1	Left	Insl
36	G_Insula-anterior-3-R	IA3R	M	SAL	37	24	0	Right	Insl
37	G_Insula-anterior-4-L	IA4L	M	SAL	-41	15	3	Left	Insl
38	G_Insula-anterior-4-R	IA4R	M	SAL	41	15	4	Right	Insl

39	G_Temporal_Sup-4-L	TS4L	L	DMN	-59	-23	4	Left	Temp
40	G_Temporal_Sup-4-R	TS4R	L	DMN	60	-20	2	Right	Temp
41	S_Sup_Temporal-1-L	ST1L	L	DMN	-50	14	-22	Left	Temp
42	S_Sup_Temporal-1-R	ST1R	L	DMN	52	13	-26	Right	Temp
43	S_Sup_Temporal-2-L	ST2L	L	DMN	-55	-7	-13	Left	Temp
44	S_Sup_Temporal-2-R	ST2R	L	DMN	54	-2	-15	Right	Temp
45	S_Sup_Temporal-3-L	ST3L	LM	DMN	-55	-33	-2	Left	Temp
46	S_Sup_Temporal-3-R	ST3R	LM	DMN	53	-32	0	Right	Temp
47	S_Sup_Temporal-4-L	ST4L	L	SAL	-57	-48	13	Left	Temp
48	S_Sup_Temporal-4-R	ST4R	L	SAL	55	-46	15	Right	Temp
49	G_Temporal_Mid-3-L	TM3L	LM	DMN	-61	-35	-5	Left	Temp
50	G_Temporal_Mid-3-R	TM3R	LM	DMN	62	-31	-5	Right	Temp
51	G_Temporal_Mid-4-L	TM4L	L	DAN	-53	-59	7	Left	Temp
52	G_Temporal_Mid-4-R	TM4R	L	DAN	57	-53	3	Right	Temp
53	G_Temporal_Inf-3-L	TI3L	M	FPN	-56	-53	-14	Left	Temp
54	G_Temporal_Inf-3-R	TI3R	M	FPN	57	-46	-14	Right	Temp
55	G_Temporal_Inf-4-L	TI4L	M	DAN	-50	-61	-8	Left	Temp
56	G_Temporal_Inf-4-R	TI4R	M	DAN	54	-58	-11	Right	Temp
57	G_Supp_Motor_Area-2-L	SMA2L	L	DMN	-11	18	61	Left	Front
58	G_Supp_Motor_Area-2-R	SMA2R	L	DMN	10	19	61	Right	Front
59	G_Supp_Motor_Area-3-L	SMA3L	LM	SAL	-7	8	64	Left	Front
60	G_Supp_Motor_Area-3-R	SMA3R	LM	SAL	6	10	65	Right	Front
61	G_Cingulum_Ant-2-L	CA2L	M	DMN	-7	34	22	Left	Lmb
62	G_Cingulum_Ant-2-R	CA2R	M	DMN	7	33	23	Right	Lmb
63	G_Cingulum_Post-2-L	CP2L	M	DMN	-4	-39	27	Left	Lmb
64	G_Cingulum_Post-2-R	CP2R	M	DMN	8	-43	31	Right	Lmb
65	G_ParaHippocampal-2-L	PH2L	M	DMN	-28	-27	-19	Left	Lmb
66	G_ParaHippocampal-2-R	PH2R	M	DMN	29	-25	-19	Right	Lmb
67	G_Fusiform-1-L	F1L	M	LIMB	-32	-9	-34	Left	Temp
68	G_Fusiform-1-R	F1R	M	LIMB	31	-8	-34	Right	Temp
69	N_Amygdala-1-L	A1L	M	DMN	-22	0	-12	Left	Lmb
70	N_Amygdala-1-R	A1R	M	DMN	21	2	-12	Right	Lmb
71	hipp_anterior_L	HAL	M	DMN	-30	-7	-19	Left	Lmb
72	hipp_anterior_R	HAR	M	DMN	30	-5	-18	Right	Lmb
73	hipp_posterior_L	HPL	M	DMN	-25	-32	-3	Left	Lmb
74	hipp_posterior_R	FS2L	M	DMN	25	-31	-2	Right	Lmb

Note: LMN: Language memory network, NTW: Network, L: Language, M: Memory, LM: Language & memory, DMN: Defult mode network, FPN: Fronto parietal network, LIMB: Limbic network, SAL: Salience network, DAN: Dorsal attention network,

Genetic algorithm feature selection

In the genetic algorithm method, each graph feature is encoded as a genome, and a subset of selected features is considered a chromosome, represented by binary strings. A uniform crossover operator with a probability of 0.6 and a mutation operator with a probability of 0.1 were used to generate new children. The accuracy of a support vector machine (SVM) classifier was used as the GA fitness function. If the generated chromosomes were the same for the last 100 generations, we stopped the process and selected the best solution (feature set) from the current population. Additionally, a maximum of 1000 generations was considered. In both methods, the selected features were based only on the training set, and only these selected features were calculated and used during testing.

Description of Cognitive Tests:

1. **Logical Memory (LM1/LM2):** This test assesses declarative/episodic memory by presenting a short story to participants, who are then asked to immediately retell it from memory. The primary performance measure is the number of story units recalled. LM is a subtest of the Revised Wechsler Memory Scale.
2. **Verbal Paired Associates (VPA1/VPA2):** VPA evaluates associative and episodic memory using word pairs. Participants hear the word pairs and respond verbally. The software automatically scores their performance.
3. **Auditory Immediate Memory (AIM):** AIM refers to the temporary storage of auditory information. It allows sounds to be held long enough for processing and understanding.
4. **Visual Immediate Memory (VI):** In neurophysiological testing, VI involves immediate recall of visual information after brief exposure.
5. **Immediate Memory (IM):** IM assesses the ability to recall information immediately after presentation.
6. **Auditory Delay (AD):** This test evaluates auditory processing and nerve conduction in the auditory pathway.
7. **Visual Delay (VD):** VD is related to visual evoked potentials (VEPs), measuring brain electrical activity in response to visual stimuli.
8. **Audio Recognition (AR):** AR assesses the ability to recognize and process sounds, a crucial aspect of auditory function. Tests like the auditory brainstem response (ABR) can measure different components of auditory processing.
9. **General Memory (GM):** GM evaluates general memory using numerical, shape patterns, or text. For instance, participants are shown a text and asked to remember it at a later time.
10. **Working Memory (WM):** WM involves holding small amounts of information actively and readily accessible for brief periods (usually less than 30 seconds). Examples include remembering a new phone number long enough to dial it or noting the date and time of an important meeting.

Table S.3: Selected features based on the GA method for LTLE and RTLE classification

fMRI				DTI			
Graph	Node name	LMN	NTW	Graph	Node name	**LMN**	**NTW**
BC	G_Angular-2-L	M	DMN	BC	G_Insula-anterior-3-L	M	SAL
BC	S_Sup_Temporal-1-R	L	DMN	BC	G_Cingulum_Ant-2-R	M	DMN
CC	S_Precentral-1-L	M	DAN	CC	G_Cingulum_Ant-2-L	M	DMN
CC	G_Temporal_Inf-3-R	M	FPN	DC	S_Sup_Frontal-2-L	M	FPN
DC	G_Frontal_Inf_Orb-1-L	L	DMN	DC	G_Insula-anterior-2-R	LM	DMN
DC	G_Parietal_Inf-1-R	M	FPN	DC	G_Temporal_Inf-3-L	M	FPN
DC	S_Intraparietal-3-L	M	DAN	DC	G_ParaHippocampal-2-L	M	DMN
DC	G_Temporal_Sup-4-L	L	DMN	LE	G_Parietal_Inf-1-L	M	FPN
DC	G_Temporal_Mid-4-R	L	DAN	LE	S_Intraparietal-2-R	M	DAN
LE	S_Precentral-1-L	M	DAN	LE	G_Temporal_Inf-4-L	M	DAN
LE	G_Supp_Motor_Area-2-R	L	DMN				
LE	G_Cingulum_Post-2-L	M	DMN				
LE	G_Fusiform-1-R	M	LIMB				

Table S.4: Selected features based on the GA method for HC and TLE classification

fMRI				DTI			
Graph	Node name	LMN	NTW	Graph	Node name	**LMN**	**NTW**
BC	G_Insula-anterior-2-L	LM	DMN	BC	G_Frontal_Inf_Tri-1-L	L	DMN
BC	G_Cingulum_Ant-2-R	M	DMN	BC	G_Cingulum_Post-2-R	M	DMN
BC	G_ParaHippocampal-2-L	M	DMN	CC	S_Precentral-4-L	LM	FPN
CC	G_Frontal_Sup-2-R	L	DMN	CC	G_SupraMarginal-7-R	L	DMN
CC	G_Insula-anterior-3-L	M	SAL	CC	G_Angular-1-L	M	DMN
CC	G_Insula-anterior-4-L	M	SAL	CC	G_Insula-anterior-4-R	M	SAL
CC	G_Supp_Motor_Area-3-R	LM	SAL	CC	G_Temporal_Mid-4-R	L	DAN
DC	G_Insula-anterior-4-L	M	SAL	CC	G_Supp_Motor_Area-3-R	LM	SAL
DC	S_Sup_Temporal-1-R	L	DMN	DC	G_Cingulum_Ant-2-L	M	DMN
DC	G_Fusiform-1-R	M	LIMB	LE	G_Fusiform-1-R	M	LIMB
DC	N_Amygdala-1-L	M	DMN				
LE	G_Cingulum_Ant-2-L	M	DMN				
LE	Hipp_anterior_R	M	DMN				

Classification evaluation metrics:

Accuracy: *Accuracy measures the overall correctness of the model's predictions as follows:*

$$\text{Accuracy} = \frac{\text{TP} + \text{TN}}{\text{Total Population}}$$

Where:

- **True Positives (TP)**: Cases correctly predicted as positive.
- **True Negatives (TN)**: Cases correctly predicted as negative.
- **Total Population**: Sum of all cases (TP + TN + FP + FN).

Sensitivity (or Recall): It measures how good a model is at identifying true positives (instances that belong to the positive class). It's calculated as:

$$\text{Sensitivity} = \frac{\text{TP}}{\text{FP} + \text{FN}}$$

Where:

- **False Negatives (FN)**: Cases incorrectly predicted as negative.

F1-Score: The F1-score is the harmonic mean of precision and recall (sensitivity). It's particularly useful when you want a balance between precision and recall, especially for imbalanced datasets. It's calculated as:

$$\text{F} - \text{Score} = 2.\frac{\text{Precision}.\,\text{Recall}}{\text{Precision} + \text{Recall}}$$

Where:

- **Precision** = True Positives / (True Positives + False Positives)

AUC (Area Under the Curve): AUC usually refers to the Area Under the Receiver Operating Characteristic (ROC) Curve. This metric assesses the performance of a classification model across all thresholds. The AUC is calculated as the integral of the curve produced by plotting the TP rate against the FP rate. An AUC score close to 1 signifies excellent model performance, while a score around 0.5 suggests the model is no better than random guessing.

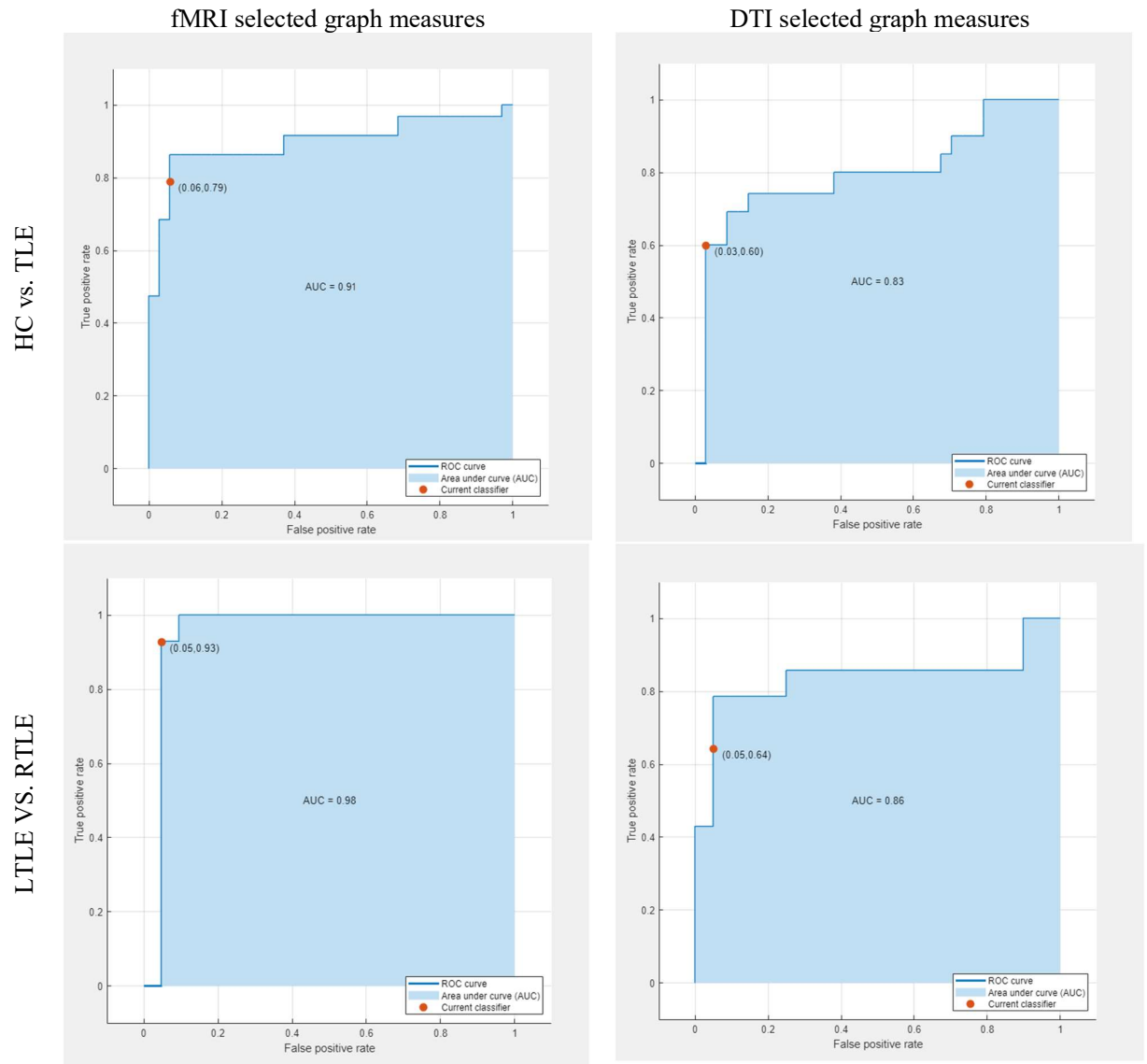

FIG S.1: The ROC plot for SVM classification result using the graph measures selected by a GA feature selection algorithm.

Completed STROBE checklist

This checklist was elaborated using formal items recommended for cross-sectional studies from the STROBE statement (https://www.strobe-statement.org).

	Item No	Recommendation	Respected?	Comments and quotes
Title and abstract	1	(*a*) Indicate the study's design with a commonly used term in the title or the abstract	Yes	The study design is indicated in the title and abstract.
		(*b*) Provide in the abstract an informative and balanced summary of what was done and what was found	Yes	This information is stated in the abstract
Introduction				
Background/rationale	2	Explain the scientific background and rationale for the investigation being reported	Yes	Rationale and existing literature are stated in the introduction section
Objectives	3	State-specific objectives, including any prespecified hypotheses	Yes	A statement at the end of the introduction specifies the specific goals and objectives.
Methods				
Study design	4	Present key elements of study design early in the paper	Yes	The study design is stated in the first subsection of the Method section.
Setting	5	Describe the setting, locations, and relevant dates, including periods of recruitment, exposure, follow-up, and data collection	Mostly	The setting, contexts, and dates of inclusion, are fully described in the method section under the "Participants" section. Locations of the data acquisition could not be disclosed due to BLINDED FOR PEER REVIEW.
Participants	6	(*a*) Give the eligibility criteria, and the sources and methods of selection of participants	Yes	The study population is described in the method section (Participants),
Variables	7	Clearly define all outcomes, exposures, predictors,	Yes	Specified in the subsections of the Method section.

		potential confounders, and effect modifiers. Give diagnostic criteria, if applicable		
Data sources/ measurement	8*	For each variable of interest, give sources of data and details of methods of assessment (measurement). Describe comparability of assessment methods if there is more than one group	Yes	Data collection and measurement were described in the "MRI Protocol and Preprocessing" of the method section. More detail was mentioned on "MRI Protocol" and "Preprocessing of Imaging Data" in the supplementary martial section.
Bias	9	Describe any efforts to address potential sources of bias	NA	Not applicable
Study size	10	Explain how the study size was arrived at	Yes	Described in the first sentence of "Participants" in the method section. The patient's demography is further described in Table S.1 of supplementary materials.
Quantitative variables	11	Explain how quantitative variables were handled in the analyses. If applicable, describe which groupings were chosen and why	Yes	Definitions of all categories for variables are presented in the subsection of the method section as follows: "- Regions of Interest (ROIs) Definition: ROI selection criteria. - Analysis of Graph Characteristics: Graph measures - Feature Selection and Classification: feature selection method and classifiers - Psychological Tests: Psychological Tests used"
Statistical methods	12	(*a*) Describe all statistical methods, including those used to control for confounding	Yes	These are described in the "Statistical Analysis" section of the Method section.
		(*b*) Describe any methods used to examine subgroups and interactions	N/A	Non applicable
		(*c*) Explain how missing data were addressed	N/A	Non applicable
		(*d*) If applicable, describe analytical methods taking account of sampling strategy	N/A	Non applicable
		(*e*) Describe any sensitivity analyses	N/A	Non applicable
Results				

Participants	13*	(a) Report numbers of individuals at each stage of study—eg numbers potentially eligible, examined for eligibility, confirmed eligible, included in the study, completing follow-up, and analysed	Yes	This is described in “Participants” subsection in the Method section
		(b) Give reasons for non-participation at each stage	N/A	Not applicable
		(c) Consider use of a flow diagram	N/A	The use of a flow diagram was not deemed appropriate
Descriptive data	14*	(a) Give characteristics of study participants (eg demographic, clinical, social) and information on exposures and potential confounders	Yes	Table 1 describes the participant's characteristics and Table S1 represents the complete information of the patients.
		(b) Indicate number of participants with missing data for each variable of interest	N/A	Not applicable
Outcome data	15*	Report numbers of outcome events or summary measures	Yes	All numbers are reported in Tables
Main results	16	(*a*) Give unadjusted estimates and, if applicable, confounder-adjusted estimates and their precision (eg, 95% confidence interval). Make clear which confounders were adjusted for and why they were included	Mostly	Fig.2 and 3 in the “Functional and Structural Connectivity Alterations in LMN” section of the result
		(*b*) Report category boundaries when continuous variables were categorized	N/A	Not applicable
		(*c*) If relevant, consider translating estimates of relative risk into absolute risk for a meaningful time period	N/A	Not applicable
Other analyses	17	Report other analyses done—eg analyses of subgroups and interactions, and sensitivity analyses	Yes	“TLE Graph Feature Selection and Classification” and “Relationship between Psychological Tests and Functional and Structural Connectivity” in the result section
Discussion				
Key results	18	Summarise key results with reference to study objectives	Yes	Key results are described in the first paragraph of the discussion section
Limitations	19	Discuss limitations of the study, taking into account	Yes	A description of limitations is done under the “Limitations”

		sources of potential bias or imprecision. Discuss both direction and magnitude of any potential bias		heading in the discussion.
Interpretation	20	Give a cautious overall interpretation of results considering objectives, limitations, multiplicity of analyses, results from similar studies, and other relevant evidence	Yes	All indicated in the Discussion.
Generalisability	21	Discuss the generalisability (external validity) of the study results	Yes	Indicated in the Discussion and Limitation.
Other information				
Funding	22	Give the source of funding and the role of the funders for the present study and, if applicable, for the original study on which the present article is based	Yes	Funding information were displayed upon submission but not included in the manuscript.

*Give information separately for exposed and unexposed groups.